

1957 UNCLASSIFIED

CONFIDENTIAL

Copy  
RM E56K09

5

NACA RM E56K09



# RESEARCH MEMORANDUM

COOLING PERFORMANCE AND STRUCTURAL RELIABILITY OF  
A MODIFIED CORRUGATED-INSERT AIR-COOLED  
TURBINE BLADE WITH AN INTEGRALLY  
CAST SHELL AND BASE

By John C. Freche and Eugene F. Schum

Lewis Flight Propulsion Laboratory  
Cleveland, Ohio

CLASSIFICATION CHANGED

UNCLASSIFIED

**LIBRARY COPY**

JAN 29 1957

LANGLEY AERONAUTICAL LABORATORY  
LIBRARY, NACA  
LANGLEY FIELD, VIRGINIA

To \_\_\_\_\_  
By authority of *NASA P.A. 3* Date *12-3-58*  
*NB 3-2-59*

CLASSIFIED DOCUMENT

This material contains information affecting the National Defense of the United States within the meaning of the espionage laws, Title 18, U.S.C., Secs. 793 and 794, the transmission or revelation of which in any manner to an unauthorized person is prohibited by law.

## NATIONAL ADVISORY COMMITTEE FOR AERONAUTICS

WASHINGTON

January 21, 1957

CONFIDENTIAL  
UNCLASSIFIED

UNCLASSIFIED



3 1176 01436 0862

## NATIONAL ADVISORY COMMITTEE FOR AERONAUTICS

RESEARCH MEMORANDUM

COOLING PERFORMANCE AND STRUCTURAL RELIABILITY OF A MODIFIED  
 CORRUGATED-INSERT AIR-COOLED TURBINE BLADE WITH  
 AN INTEGRALLY CAST SHELL AND BASE

By John C. Freche and Eugene F. Schum

## SUMMARY

An investigation was conducted in a turbojet engine modified for air-cooling to evaluate a light air-cooled blade with augmented internal heat-transfer surface area and an integrally cast shell and base. This blade, which has 0.050-inch corrugations brazed to the shell and to an island in the base, weighs approximately the same as conventional corrugated-insert blades with sheet-metal shells.

Heat-transfer data at rated engine conditions indicated a fairly uniform temperature distribution at the critical 1/3-span section. At a coolant-flow ratio of 0.0135, the maximum temperature reduction of this spanwise location from effective gas temperature (1462° F) was 282° for a blade cooling-air inlet temperature of 249° F. Because of reduced flow area, the cooling-air pressure drop of the blade was 2 to  $2\frac{1}{2}$  times that of a conventional corrugated-insert blade with the same size corrugations. This pressure drop does not appear excessive compared with the pressure difference available when cooling air is supplied from compressor bleed.

Three HS-31 modified corrugated-insert blades were endurance-operated without failure for 16, 31, and 36 hours at a 1/3-span temperature of 1375° F and stress of 28,700 psi. Inlet gas temperatures ranged from 1600° to 1670° F and coolant-flow ratios from 0.0064 to zero. A fourth blade (HS-21) failed after 15 hours at the 1/3 span, failure probably being initiated at a surface instrumentation slot. Calculations indicate that a coolant-flow ratio of approximately 0.036 is required to maintain an average 1/3-span shell temperature of 1375° F in the application of this type blade to a turbojet engine at a Mach number of 2, an altitude of 50,000 feet, and an inlet gas temperature of 2500° F. If local temperatures greatly exceed the average temperature specified, larger coolant-flow ratios may be required.

UNCLASSIFIED

~~CONFIDENTIAL~~

## INTRODUCTION

Air-cooled turbine rotor blades have been under investigation at the NACA Lewis Laboratory for several years. The results of cooling and of endurance investigations of various shell-supported and strut-supported air-cooled blades are summarized in references 1 to 6. The shell-supported blades were generally lightweight and usually consisted of three main components: a cast base, a formed hollow shell, and tubes or fins inserted into the hollow shell to increase the coolant heat-transfer surface area. These components were brazed together.

In order to provide an alternate method of manufacture, a completely cast blade in which large numbers of small coolant passages were cast near the surface of the airfoil was developed (ref. 7). This method of manufacture reduced the number of blade component parts and eliminated the brazed joint between blade shell and blade base. British investigators experimented with cast and sintered blades (refs. 8 and 9, respectively) and with fully forged blades having similar cooling configurations (ref. 10). Local stress concentrations due to thermal gradients between the coolant passages and the blade surface may be a problem with this type of blade. An additional undesirable feature of this blade is its relatively high weight, which can be reduced by making the tip section hollow, as described in reference 7.

Another method of reducing blade weight while utilizing an integral shell and base casting was evolved and resulted in the modified corrugated-insert blade reported herein. In this modified corrugated-insert blade the cooling airflow is confined to the coolant passages formed by the inner walls of the blade shell and corrugations brazed to the shell. The sheet-metal insert, which usually (in a conventional corrugated-insert blade) is brazed to the inner surface of the corrugations to permit cooling airflow past both sides of the corrugations, is omitted. As a result, this blade has half the free flow area for the coolant that a conventional corrugated-insert blade has. Heat-transfer theory indicated that the modified corrugated-insert blade could not be cooled as effectively as the conventional corrugated-insert blade. Because of its smaller number of blade components, which in turn might serve to simplify blade fabrication, it was considered desirable to obtain heat-transfer and endurance data with the modified corrugated-insert blade. Furthermore, the structural reliability results obtained may be applied (for the same blade shell temperature) to a similarly cast integral shell and base blade with a conventional corrugation installation.

The investigation described herein was of an exploratory nature, designed to show whether or not the modified corrugated-insert blade warranted further development. Consequently, as a means of simplification the tests were limited to a few (four) blades and current gas temperature levels. This report presents (1) experimental cooling results, (2) verification of a method of calculating blade temperature, and (3) structural reliability results.

The modified corrugated-insert turbine blades were operated at sea-level ambient conditions in a turbojet engine altered to accommodate two air-cooled blades. Heat-transfer data were obtained over a range of cooling-air flows at constant engine speeds of 10,000 and 11,500 rpm (rated speed). The range of gas-to-blade Reynolds numbers (based on film temperature and a nondimensional term, perimeter divided by  $\pi$ ) at the rotor blade inlet was 183,500 to 217,000. Coolant- to gas-flow ratios ranged from 0.0023 to 0.0166. Structural reliability tests were made at rated engine speed (1/3-span centrifugal stress of 27,770 and 28,700 psi, depending on blade material) and inlet gas temperatures of 1670° and 1600° F, with corresponding coolant-flow ratios of 0.0064 and zero, respectively.

## APPARATUS AND INSTRUMENTATION

### Air-Cooled Turbine Blades

The air-cooled blades investigated had a span and chord of approximately 4 and 2 inches, respectively, and were twisted from root to tip. Sections through the blade are shown in figure 1. The blade shell was cast integrally with the base. High-temperature alloys with good casting properties were chosen. One blade was cast from HS-21 alloy and three were cast from HS-31 (X-40) alloy. The shell was cast with a taper, being 0.020 inch thick at the tip and 0.070 inch thick at the root. To provide additional structural rigidity, an island (see fig. 1) was cast integrally with the blade base. This island extended upward from the base approximately 3/8 inch into the hollow blade shell.

Each row of corrugations (A-286 material of approximately 0.050-in. pitch, 0.050-in. amplitude, and 0.005-in. thickness) was inserted from the blade tip and was brazed to one side of the blade as well as to the island. The corrugations extended approximately 1/16 inch below the blade base platform. The openings between corrugation and island were intentionally blocked (see fig. 1). At the leading and trailing edges the two rows of corrugations extended beyond the front and back edges of the island. In these regions the space between the two corrugation rows was filled with braze, as shown in section A-A of figure 1. Thus, cooling air was permitted to flow only through the spaces between the shell and the corrugations. The blade profile was identical to that of the cast-cored blade (ref. 7), the same casting dies having been used.

### Engine Modifications

The engine modifications are described in detail in reference 11. For cooled operation, an external source (laboratory service air system) supplied the blade cooling air, which was ducted through two tubes

fastened to the rotor rear face and through passages drilled transversely through the rotor rim beneath the test blades. Two cooled test blades were located diametrically opposite each other in the rotor, and the rotor assembly was completed with 52 standard uncooled S-816 blades. Thus, it was possible to investigate two cooled blades simultaneously. An adjustable tailpipe nozzle was provided for the test engine so that the turbine-inlet temperature could be varied at a given engine speed.

### Blade and Engine Instrumentation

For heat-transfer investigations two of the test blades were instrumented with thermocouples as shown in figure 2. These thermocouples were buried in the blade shell by the method described in reference 12. Endurance operation was also initiated with these two blades. As the endurance running progressed, repeated thermocouple failures were encountered and the number of thermocouples was reduced. In order to provide reference temperatures for use in setting the endurance operating conditions, thermocouples were installed in the leading edge at approximately the root and 1/3-span positions; one thermocouple was also provided at the root midchord suction surface. These thermocouples were attached to the blades by employing a simplified installation technique. The tubes enclosing the thermocouple leads were strapped to the blade surface rather than inserted into grooves in the blade surface, as was the case for the heat-transfer test thermocouple installation. In all cases the thermocouple junction was embedded immediately beneath the blade surface.

Two standard uncooled blades (reference blades) were each provided with a thermocouple at the leading edge, approximately at the 1/3-span position, to measure the effective gas temperature. The reference blades were cut off at the 2/3-span position as shown in figure 2. By reducing the centrifugal stress of the reference blades the possibility of early failure due to metal removal for thermocouple installation was reduced. Engine speed, airflow, fuel flow, cooling airflow and temperature, and tailpipe gas temperature were all measured as described in reference 11.

### PROCEDURE

#### Heat-Transfer Investigation

Blade cooling effectiveness was determined in a manner similar to that described in reference 11. Blade temperature data were obtained at engine speeds of 10,000 and 11,500 rpm (rated) and at effective gas temperatures (reference blade temperature) of 1130° and 1462° F. Coolant-to-gas flow ratio (hereinafter called coolant-flow ratio) was varied at each engine speed over as wide a range as the experimental installation permitted. The coolant-flow-ratio range extended from 0.0032 to 0.0166

at 10,000 rpm and from 0.0023 to 0.0135 at 11,500 rpm. The blade pressure drop and the service air supply to the test installation limited the coolant-flow range. The values presented consider the quantity of coolant leakage between stationary and rotating parts of the cooling-air system at the rotor hub as determined by a separate calibration as in reference 5. The heat-transfer operating data are presented in table I.

### Structural-Reliability Investigation

The structural reliability of one cast HS-21 and three cast HS-31 modified corrugated-insert blades was determined by engine operation at rated conditions. The calculated blade root centrifugal stress was 33,100 psi and the 1/3-span stress was 28,700 psi for the HS-31 blades, and slightly lower for the HS-21 blade. The operating conditions are summarized in table II. Three of the blades were operated with a coolant-flow ratio of 0.0064, and one was operated uncooled. During uncooled operation the average 1/3-span blade temperature was maintained equal to its value (1375° F) under cooled operating conditions by reducing the inlet gas temperature slightly. In order to reduce total operating time, endurance runs were limited to time values that provided reasonably low but not the minimum allowable- to centrifugal-stress ratio. This is discussed more fully in a subsequent section.

### Blade Pressure-Drop Determination

The mockup section of the turbine rotor instrumented as described and illustrated in figure 10(a) of reference 13 was used to obtain the static-pressure drop through the research blade (shell and base). The pressure drop was determined for a range of air weight flows from 0.0029 to 0.0373 pound per second in several increments.

## CALCULATIONS

### Heat-Transfer Calculations

The average blade shell temperature at the 1/3 span was calculated from the following equation (eq. (18) of ref. 14):

$$\frac{T_{g,e} - T_b}{T_{g,e} - T_{a,e,r}} = \frac{1}{1 + \lambda} e^{-\left(\frac{1}{1+\lambda} \frac{h_o l_o b}{c_p w_a} \frac{y}{b}\right)} - \frac{\omega^2 w_a b}{g J h_o l_o (T_{g,e} - T_{a,e,r})} \frac{y}{b} + \left[ 1 - e^{-\left(\frac{1}{1+\lambda} \frac{h_o l_o b}{c_p w_a} \frac{y}{b}\right)} \right] \left[ \frac{\omega^2 w_a}{g J h_o l_o (T_{g,e} - T_{a,e,r})} \right] \left[ \frac{c_p w_a (1 + \lambda)}{h_o l_o} - r_r \right] \quad (1)$$

(All symbols are defined in appendix A.) The local gas-to-blade heat-transfer coefficients were theoretically determined by the method of reference 15 and averaged to obtain the  $h_o$  used in calculating blade temperatures. The blade velocity profiles required in this determination were obtained from stream-filament theory as described in reference 16.

The effective gas temperature  $T_{g,e}$  for use in equation (1) was obtained from a correlation of the measured effective gas temperature and unpublished NACA data by averaging the spanwise effective gas temperature profile previously measured in this engine.

The effective blade-to-coolant heat-transfer coefficient  $h_f$  was determined from the following equation, which is derived in appendix B:

$$h_f = \frac{h_1}{\tau + m} \left[ \frac{\tanh\left(L \sqrt{\frac{h_1}{k\tau}}\right)}{\sqrt{\frac{h_1}{k\tau}}} + m \right] \quad (2)$$

and the heat-transfer correlations expressed in figure 2 of reference 17. In this reference, in which the coolant properties were evaluated at a film temperature, the correlation is given for laminar, transition, and fully developed turbulent flow. In these calculations the appropriate flow range was employed depending on the Reynolds number involved. The calculated average 1/3-span temperatures were then compared with arithmetically averaged experimental values obtained at the same station over a range of coolant-flow ratios.

#### Stress Calculations

The controlling blade stress was considered to be centrifugal. Stress calculations were made for the 1/3-span position and were based upon the shell and corrugation metal cross-sectional area. The centrifugal stress at the root region of the shell was similarly calculated. The supporting effect of the island on the corrugations was not considered in the stress calculation.

The allowable blade stress was determined from the average blade temperature at the 1/3-span position and stress-rupture data for the blade materials (HS-21 and HS-31). The ratio of allowable to centrifugal stress was determined for each of the blades investigated for the period of time accumulated at rated test conditions.

## RESULTS AND DISCUSSION

### Experimental Results

Heat transfer. - The blade heat-transfer data are given in table I. Chordwise blade temperature distributions are shown in figure 3 for the 1/3-span position. Figure 3(a) shows several typical blade temperature-distribution curves for the 10,000-rpm runs, and figure 3(b) shows the temperature-distribution curves for rated engine speed obtained at each coolant-flow ratio. The effective gas temperature (uncooled solid blade temperature) at the 1/3 span is also included on the figure. Since the cooling-air temperatures at the blade inlet vary with coolant-flow ratio, they cannot conveniently be shown in the figure. These values are listed in table I.

At both engine speeds the shape of the temperature-distribution curves changes markedly with increasing coolant-flow ratio. At the higher flow ratios the curves tend to assume a more conventional shape, showing midchord temperatures lower than leading- and trailing-edge temperatures. Regardless of coolant-flow ratio, however, the blade operated at a fairly uniform chordwise temperature at the 1/3-span position. At rated engine speed and a coolant-flow ratio of 0.0135, the maximum temperature reduction from effective gas temperature was 282° and occurred at the midchord suction surface. The blade cooling-air inlet temperature for this condition was 249° F. Induced thermal stresses caused by chordwise temperature gradients in this critically stressed region are thus kept to a minimum. The fairly uniform (maximum difference, 55°) chordwise temperature distribution is probably due to a uniform coolant-flow distribution brought about by the favorable cooling-air entrance configuration in the base (fig. 1) as well as the relatively high blade pressure drop.

Figure 3 indicates that the 10,000-rpm data were obtained with all the thermocouples intact, whereas the rated-speed temperature-distribution curves were faired in at the leading-edge region because of failure of the leading-edge thermocouple. The fairing did not follow the trends indicated by the 10,000-rpm data, which showed measured leading-edge temperatures lower than trailing-edge temperatures. Instead, the rated-speed curves were completed by making the leading-edge temperature equal to the trailing-edge temperature. This resulted in a higher average blade temperature; however, the trend is more in keeping with results obtained with other cooled blades.

The nondimensional blade cooling-effectiveness parameter  $\phi$  obtained by using the average 1/3-span blade temperature is plotted against coolant-flow ratio for constant engine speed (constant mass flow) in figure 4. All the heat-transfer runs at both speeds are represented here. As might be expected, the blade cooling effectiveness increases with increasing coolant-flow ratio. It also increases with decreasing engine speed, as a result of the lower outside heat-transfer coefficient associated with the reduced engine mass flow at the lower engine speed. With these effectiveness curves it is possible to determine the blade temperature at any coolant-flow ratio for similar engine mass flows. It is not advisable, however, to extrapolate these results to gas temperatures many hundreds of degrees in excess of the gas temperature level at which these data were obtained.

The blade root temperatures obtained may be seen in table I. Only limited instrumentation was applied at this spanwise station, since it is not the critical blade section. These temperatures are of some interest because the blade centrifugal stress is a maximum at the root. At an approximate coolant-flow ratio of 0.010 the root temperatures are about 200° below the 1/3-span temperatures at rated engine speed, a fact which tends to compensate for the higher root stress level by providing improved material strength properties.

Calculated and experimental blade temperatures. - Calculated and experimental 1/3-span average blade temperatures are compared in figure 5 at rated speed and a turbine-inlet gas temperature of 1670° F. The coolant-flow-ratio range covered was from 0.0023 to 0.0135. Deviation of a line drawn through the plotted points from a 1-to-1 correlation line is 70°; the maximum deviation of a calculated temperature from an experimental temperature was 130° F, occurring at an experimental temperature of 1380° F. The data were calculated assuming that all cooling-air leakage was accounted for. The leakage calibration cannot be conducted with the test blade, but requires that a standard uncooled blade be used. Consequently, inevitable machining differences in the base serrations of the two blades can cause a small error in the leakage determination. This effect coupled with the possibility of inaccuracies due to idealization in the heat-transfer theory could account for differences between calculated and experimental temperatures.

An additional blade temperature calculation was made using an average gas-to-blade heat-transfer coefficient obtained from the correlation of experimental heat-transfer data for a blade of similar shape shown in reference 10. The gas-to-blade heat-transfer data of the reference agreed within 15 percent with the coefficients determined by the method of reference 15. This 15-percent difference had only a negligible effect on calculated blade temperature, about 29° F in 1244° F.

Structural reliability. - Structural-reliability data are summarized in table II. One of four blades tested failed at the 1/3 span (centrifugal stress, 27,770 psi) after approximately 15 hours of engine operation at rated conditions. About 10 hours of additional operation were compiled with this blade at lower speeds and other coolant-flow ratios during the heat-transfer runs. The failed blade was of HS-21 material and is shown in figure 6. It is likely that the instrumentation grooves on the blade surface contributed to the early blade failure. Metallurgical examination indicated that failure could have been initiated in the leading-edge region at the location of a slot used for installing the leading-edge thermocouple.

The remaining three blades (HS-31 material) were operated without major blade failure for approximately 16, 31, and 36 hours at rated engine conditions. Portions of the corrugations near the tip in two of the blades were thrown clear during the runs without otherwise damaging the blades, and the durability tests were continued without ill effects. The corrugation loss was due to an unsatisfactory braze between the corrugations and the shell. During endurance operation with two of these blades, the coolant-flow ratio was held at 0.0064. This is approximately the minimum value that can be accurately maintained over extended periods in the test installation. The average 1/3-span blade temperature was 1375° F under these conditions. The third blade was operated at rated speed uncooled in order to eliminate the need for repeated blade instrumentation, thereby expediting the test. During uncooled operation, the 1/3-span blade temperature was maintained at 1375° F by lowering the inlet gas temperature to 1600° F.

The ratios of allowable to centrifugal stress (stress-ratio factor) obtained are plotted against the operating time for each blade in figure 7. The small arrows above the individual data points in the figure indicate whether further operation was possible. The curves were extended (dashed lines in fig. 7) by calculating the blade stress-ratio factor at various time intervals up to 100 hours. The extension of these curves shows that further appreciable reduction in stress-ratio factor could be achieved only by extensive operation. Since visual inspection of the HS-31 blades showed no sign of impending failure, operation was terminated. The limiting stress-ratio factor was not determined for the HS-31 blades, since no failure occurred. As for the HS-21 blade, the presence of instrumentation slots on the blade surface probably contributed to the early failure, so that a true stress-ratio factor was not determined in this case.

Although only a limited number of blades was investigated, no failures of the shell in the highly stressed root region were encountered. These results show promise that the integral shell and base type of construction affords adequate strength for high-centrifugal-stress operation.

Blade cooling-air pressure drop. - The cooling-air pressure drop through the blade was obtained over a range of coolant flows from approximately 0.003 to 0.036 pound per second. The pressure drop of the modified corrugated-insert blade is discussed in the following section, where it is compared with the pressure drop obtained for several other air-cooled blades.

#### Comparisons with Other Blades

Temperature. - One basis for determining the potential of the modified corrugated-insert blade is a temperature comparison of the stress-supporting member at the critical section with other air-cooled configurations. Figure 8 shows the change in average 1/3-span blade temperature with coolant-flow ratio for the modified corrugated-insert blade, a conventional corrugated-insert blade (similar to the type described in ref. 4) with 0.050-inch corrugations, and the cast-cored blade reported in reference 7. The temperature curves for the latter two blades were calculated, that for the conventional corrugated-insert blade by the method of reference 14 using blade-to-coolant coefficients obtained as described in reference 17.

The blade temperature shown for the cast-cored blade represents an average of the surface- and central-region temperatures, because both regions help support the blade load (ref. 7). Since the central region in this type of blade is similar to the strut in a strut-supported blade, its temperature is very low, and the resultant average temperature is low. At a coolant-flow ratio of 0.015, the modified corrugated-insert blade temperature is about 210° F (17.5 percent) higher than that of the cast-cored blade.

The modified corrugated-insert blade temperature is also higher than that of the conventional corrugated-insert blade. For example, at an 0.015 coolant-flow ratio it was 225° F, or 19 percent, higher. These results might generally be expected because heat-transfer theory indicated that the conventional corrugated-insert blade would cool more effectively than the modified corrugated-insert blade owing to its greater heat-transfer surface area. However, the investigation was primarily conducted as an exploratory venture for the reasons previously discussed (i.e., smaller number of blade components, etc).

Blade weight. - The modified corrugated-insert blade weighs slightly over 0.68 pound. Reference 7 shows that a simple hollow blade for this engine application weighs 0.66 pound, a conventional corrugated-insert blade 0.68 pound, the cast blade with cooling passages running the entire blade length (cast-cored blade) 0.82 pound, and the cast-cored blade with a hollow tip section 0.74 pound. Thus, the modified corrugated-insert blade configuration is on a par with a conventional corrugated-insert blade

and very closely approaches the hollow blade, which may be regarded as a minimum blade weight. Examination of the modified corrugated-insert blade indicates that it has only two more structural components than exist in a hollow blade, namely, the corrugations and the island insert, which are both extremely light members. Thus, added heat-transfer surface and structural stability are supplied in this design at a minimum cost in weight. At the same time, the integral construction of base and shell avoids dependence upon a brazed joint for carrying the major blade load.

Blade cooling-air pressure drop. - Figure 9 presents the cooling-air pressure drop through the modified corrugated-insert blade, the cast-cored blade of reference 7, and a conventional corrugated-insert blade with 0.050-inch corrugations over a coolant-flow range of approximately 0.003 to 0.050 pound per second. The values shown are average values, since the pressure drop through individual cooling passages was not measured. Over the coolant-flow range shown, the modified corrugated-insert blade shows a pressure drop approximately  $2\frac{1}{2}$  to  $4\frac{1}{2}$  times that of the cast-cored blade and 2 to  $2\frac{1}{2}$  times that of the conventional corrugated-insert blade. Because of the small coolant-flow area in the modified corrugated-insert blade, high pressure drop relative to these other blades is to be expected. The magnitude of pressure drop that is acceptable depends, of course, upon the engine application under consideration. For example, at a coolant flow of 0.013 pound per second a 7.3-pound-per-square-inch pressure drop results with the modified corrugated-insert blade. This pressure loss does not appear to be excessive compared with the pressure difference available when cooling air is supplied from compressor discharge bleed; however, the conditions of the specific installation must be the determining factor. Since the blade pressure drop was determined in a stationary installation at room temperature, the effects of rotation and coolant temperature rise are not included in these results. The values presented nevertheless indicate the blade pressure losses on a qualitative basis.

#### Potential of Modified Corrugated-Insert Blade

In order to evaluate the potential of the modified corrugated-insert blade more fully, its cooling requirements in high gas temperature, high altitude, and high flight Mach number applications must be known. The coolant-flow ratios required for this blade were calculated for a single-stage-turbine application in a turbojet engine operating at a flight Mach number of 2, an altitude of 50,000 feet, and over a range of inlet gas temperatures from 2000° to 2500° F. Similar calculations are made for conventional corrugated-insert blades at elevated conditions in reference 18 and for the cast-cored blade in reference 7.

4284

CU-2 back

In calculating the cooling requirements of the modified corrugated-insert blade, both 1375° and 1148° F average blade temperatures were specified at the 1/3-span position. The former value was chosen since reasonable blade life was obtained while maintaining this temperature during blade durability tests. The latter value was the same as that specified in similar calculations for the cast-cored blade (ref.-7), thus permitting a comparison. Values of gas-to-blade heat-transfer coefficients were estimated from reference 19. An engine with a sea-level compressor pressure ratio of 4 and corrected engine weight flow per unit frontal area of 25.5 pounds per second per square foot was assumed. Blade cooling-air inlet temperature was considered to be 588° F (compressor bleed temperature plus 100° F). Equation (1) was employed. To account for the inaccuracies demonstrated in calculating blade temperatures at rated engine operating conditions, the ratio of the experimental to the calculated blade temperature values obtained at rated engine conditions was incorporated in these calculations.

Figure 10 shows the calculated required coolant-flow ratio as the inlet gas temperature is increased from 2000° to 2500° F for both the modified corrugated-insert and the cast-cored blades. To maintain the average 1/3-span modified corrugated-insert blade temperature at 1375° F, the coolant-flow ratio required varies from 0.020 at a 2000° F gas temperature to 0.0355 at a 2500° F gas temperature. These flow requirements are approximately doubled when the average 1/3-span blade temperature is reduced to 1148° F. Figure 10 also shows that the modified corrugated-insert blade requires coolant-flow ratios about twice as large as the cast-cored blade over the entire gas temperature range considered to maintain an average 1/3-span blade temperature of 1148° F. All the curves fall within the calculated coolant-flow-ratio range tabulated in reference 18 as the limitations of 80 corrugated-insert blade designs. The blade designs considered in reference 18 were not limited on the basis of cooling-air pressure drop. This may not be the case for the modified corrugated-insert blade, however. It should also be noted that this calculation presumes that the chordwise temperature differences will not differ markedly from experimental results at rated engine operating speed. Of course, it is possible that the leading-edge temperature can considerably exceed the specified average blade temperature at higher gas temperature levels. In such a case larger coolant-flow ratios may be required to overcome the effects of such local hot spots.

The present investigation indicates a means for combining reasonable blade performance with light weight. More effective heat transfer and lower cooling-air pressure drops may be achieved merely by using corrugations in the conventional manner without noticeably affecting weight or altering the basic design precept of nondependence on brazed joints for major load support.

## SUMMARY OF RESULTS

The following results were obtained from an experimental investigation of a modified corrugated-insert air-cooled blade:

1. The modified corrugated-insert blade shows a fairly uniform temperature distribution at the critical 1/3-span section. The maximum reduction from effective gas temperature (1462° F) obtained at this spanwise location and a rated engine operating condition was 282°, occurring at a coolant-flow ratio of 0.0135. The coolant temperature at the blade inlet was 249° F.

2. A static room-temperature blade cooling-air pressure-drop determination showed the modified corrugated-insert blade to have a pressure drop  $2\frac{1}{2}$  to  $4\frac{1}{2}$  times that of a cast-cored blade and 2 to  $2\frac{1}{2}$  times that of a conventional corrugated-insert blade with the same size corrugations. This pressure drop does not appear to be excessive compared with the pressure difference available when cooling air is supplied from compressor bleed.

3. Three HS-31 modified corrugated-insert blades with A-286 corrugations were endurance-operated at a 1/3-span stress of 28,700 psi, rated engine speed, and inlet gas temperatures of 1670° and 1600° F for approximately 16, 31, and 36 hours without blade failure. Two of these blades were operated at a 0.0064 coolant-flow ratio and one with zero coolant flow while maintaining a 1/3-span average shell temperature of 1375° F. One HS-21 blade with A-286 corrugations failed at the 1/3 span, failure probably being initiated at a surface instrumentation slot after about 15 hours at rated conditions and 0.0064 coolant-flow ratio.

4. Calculations indicate that a modified corrugated-insert blade would require a coolant-flow ratio of approximately 0.036 to maintain an average 1/3-span shell temperature of 1375° F, assuming the blade to be employed in a turbojet engine at an inlet gas temperature of 2500° F, an altitude of 50,000 feet, and a Mach number of 2. If local temperatures such as the leading edge greatly exceed the average temperature specified at these higher gas temperature levels, larger coolant-flow ratios may be required.

5. Modified corrugated-insert blade weight (about 0.68 lb) was approximately the same as that of a conventional corrugated-insert blade and only slightly heavier than a simple hollow blade (0.66 lb).

Lewis Flight Propulsion Laboratory  
National Advisory Committee for Aeronautics  
Cleveland, Ohio, November 13, 1956

## APPENDIX A

## SYMBOLS

A	fin cross-sectional area, $C_{xt}$ , sq ft
B	location on fin where $\frac{dT}{dx} = 0$ (see fig. 11(a)), ft
b	blade height or span, 0.333, ft
C	length of fin spanwise to blade (see fig. 11(b)), ft
$c_p$	specific heat at constant pressure, Btu/(lb)(°F)
g	acceleration due to gravity, 32.2 ft/sec <sup>2</sup>
H	constant
h	heat-transfer coefficient, Btu/(sec)(sq ft)(°F)
$h_f$	effective inside heat-transfer coefficient, Btu/(sec)(sq ft)(°F)
J	mechanical equivalent of heat, 778 ft-lb/Btu
K	constant
k	thermal conductivity of equivalent fin, Btu/(sec)(ft)(°F)
L	length of equivalent fin normal to shell, 0.0043 ft (see fig. 11(b))
z	blade perimeter, ft
m	distance between equivalent fins, 0.00375 ft (see fig. 11(b))
p	static pressure, lb/sq in.
Q	quantity of heat transferred per second, Btu/sec
r	radius, ft
T	temperature, °F
w	weight flow, lb/sec
x	distance along equivalent fin in direction L to fin element, ft

y distance from blade root to spanwise station considered, ft

$$\beta \sqrt{\frac{h_i C}{kA}}, \frac{1}{ft}$$

$$\lambda \frac{h_o l_o}{h_f l_s}$$

$\rho$  density, lb/cu ft

$\tau$  thickness of equivalent fin, 0.000416 ft

$\phi$  cooling-effectiveness parameter,  $\frac{T_{g,e} - T_b}{T_{g,e} - T_a}$

$\omega$  angular velocity, radians/sec

Subscripts:

a blade cooling air

b blade

c corrugation

e effective

f fin

g combustion gas

i inside

o outside

r blade root

s portion of blade inner surface adjacent to air passages formed by corrugations

std standard atmosphere

## APPENDIX B

## DERIVATION OF EFFECTIVE BLADE-TO-COOLANT HEAT-TRANSFER COEFFICIENT

In order to solve equation (1), it is necessary to substitute an effective blade-to-coolant heat-transfer coefficient  $h_f$  in the  $\lambda$  term. The effective coefficient is one that accounts for the additional heat-transfer surface area supplied by the corrugations, thus permitting expression of the heat transferred to the cooling air in terms of the blade-shell to cooling-air temperature difference. To facilitate an analysis of the heat-transfer process, the corrugations may be replaced by an equivalent simplified configuration. The numerical values of the fin dimensions used in the temperature calculations are given in appendix A. These were average values determined from a sectioned blade by measurements made with a microscope. Figure 11(a) shows a section of the blade shell with attached corrugations, and figure 11(b) shows how the corrugations may be replaced by fins extending from the shell at right angles. Figure 11(c) illustrates how the cooling action of each corrugation or substituted fin is replaced by a heat-transfer coefficient,  $h_c$ . The effective or over-all heat-transfer coefficient  $h_f$ , which includes the effects of  $h_c$  and  $h_1$ , is derived as follows.

Writing a heat balance for such an equivalent fin as shown in figure 11(b) results in the differential equation

$$kA \frac{d^2 T_f}{dx^2} - h_1 T_f C = -h_1 T_a C \quad (B1)$$

The general solution for this equation is

$$T_f = H e^{\beta x} + K e^{-\beta x} + T_a \quad (B2)$$

as shown in reference 20. The term  $\beta$  is defined in appendix A.

One of the constants can be eliminated from equation (B2) by substituting the boundary condition of  $dT_f/dx = 0$  at  $x = L$  (station B of fig. 11(a)) after differentiating the equation with respect to  $x$ . This results in

$$T_f = H(e^{\beta x} + e^{2\beta L - \beta x}) + T_a \quad (B3)$$

The temperature at the intersection of the fin and the shell may then be represented by substituting 0 for  $x$  in equation (B3), thereby obtaining

$$T_{f_{x=0}} = T_b = H(1 + e^{2\beta L}) + T_a \quad (B4)$$

Using these equations to relate the amount of heat transferred by conduction into the fins through the cross-hatched area (fig. 11(c)) to that being transferred to the coolant by the coefficient  $h_c$  which replaces the corrugation (see fig. 11(c)) results in

$$Q = h_c C \tau (T_b - T_a) = -k C \tau \left( \frac{dT_f}{dx} \right)_{x=0} \quad (B5)$$

The value of  $dT_f/dx$  for  $x=0$  for substitution into equation (B5) is obtained by differentiating equation (B3). The value of  $T_b$  at the intersection of the fin and shell as expressed by equation (B4) is also substituted into equation (B5). This results in an equation from which  $h_c$  can be evaluated:

$$h_c = - \sqrt{\frac{kh_1}{\tau}} \left( \frac{1 - e^{-2L\sqrt{h_1/k\tau}}}{1 + e^{-2L\sqrt{h_1/k\tau}}} \right) \quad (B6)$$

which in hyperbolic form is

$$h_c = \sqrt{\frac{kh_1}{\tau}} \tanh \left( L \sqrt{\frac{h_1}{k\tau}} \right) \quad (B7)$$

The effective blade-to-coolant coefficient  $h_f$  equals an average of the individual blade-to-coolant coefficients (fig. 11(c)) on an area basis:

$$h_f = \frac{h_c \tau_c + h_1 m}{\tau_c + m} \quad (B8)$$

By substituting the hyperbolic relation for  $h_c$  (eq. (B7)) into equation (B8), the final form for evaluating the effective heat-transfer coefficient is obtained:

$$h_f = \frac{h_1}{\tau_c + m} \left[ \frac{\tanh \left( L \sqrt{\frac{h_1}{k\tau}} \right)}{\sqrt{\frac{h_1}{k\tau}}} + m \right] \quad (2)$$

## REFERENCES

1. Esgar, J. B., Livingood, J. N. B., and Hickel, R. O.: Research on Application of Cooling to Gas Turbines. Paper No. 56-SA-54, ASME, 1956.
2. Hickel, Robert O., and Ellerbrock, Herman H., Jr.: Experimental Investigation of Air-Cooled Turbine Blades in Turbojet Engine. II - Rotor Blades with 15 Fins in Cooling-Air Passages. NACA RM E50I14, 1950.
3. Smith, Gordon T., and Hickel, Robert O.: Experimental Investigation of Air-Cooled Turbine Blades in Turbojet Engine. V - Rotor Blades with Split Trailing Edges. NACA RM E51A22, 1951.
4. Bartoo, Edward R., and Clure, John L.: Experimental Investigation of Air-Cooled Turbine Blades in Turbojet Engine. XIII - Cooling Effectiveness of a Blade with an Insert and with Fins Made of a Continuous Corrugated Sheet. NACA RM E52F24, 1952.
5. Stepka, Francis S., Bear, H. Robert, and Clure, John L.: Experimental Investigation of Air-Cooled Turbine Blades in Turbojet Engine. XIV - Endurance Evaluation of Shell-Supported Turbine Rotor Blades Made of Timken 17-22A(S) Steel. NACA RM E54F23a, 1954.
6. Schum, Eugene F., Stepka, Francis S., and Oldrieve, Robert E.: Fabrication and Endurance of Air-Cooled Strut-Supported Turbine Blades with Struts Cast of X-40 Alloy. NACA RM E56A12, 1956.
7. Freche, John C., and Oldrieve, Robert E.: Fabrication Techniques and Heat-Transfer Results for Cast-Cored Air-Cooled Turbine Blades. NACA RM E56C06, 1956.
8. Glenny, E.: The Application of the Investment-Casting Technique to the Manufacture of Blade Shapes Containing Cooling Fluid Passages. Memo. No. M.122, British N.G.T.E., Dec. 1951.
9. Ainley, D. G., Waldren, N. E., and Hughes, K.: Investigations on an Experimental Air-Cooled Turbine. II - Cooling Characteristics of Blades Having a Multiplicity of Small Diameter Coolant Passages. Rep. No. R.154, British N.G.T.E., Mar. 1954.
10. Ainley, D. G.: The High Temperature Turbo-Jet Engine. Jour. Roy. Aero. Soc., vol. 60, no. 549, Sept. 1956, pp. 563-581; discussion, pp. 581-589.

11. Ellerbrock, Herman H., Jr., and Stepka, Francis S.: Experimental Investigation of Air-Cooled Turbine Blades in Turbojet Engine. I - Rotor Blades with 10 Tubes in Cooling-Air Passages. NACA RM E50I04, 1950.
12. Stepka, Francis S., and Hickel, Robert O.: Methods for Measuring Temperatures of Thin-Walled Gas-Turbine Blades. NACA RM E56G17, 1956.
13. Schafer, Louis J., Jr., and Hickel, Robert O.: Analytical Determination of Effect of Turbine Cooling-Air-Impeller Performance on Engine Performance and Comparison of Experimentally Determined Performance of Impellers with and without Inducer Vanes. NACA RM E54H12, 1954.
14. Livingood, John N. B., and Brown, W. Bryon: Analysis of Spanwise Temperature Distribution in Three Types of Air-Cooled Turbine Blades. NACA Rep. 994, 1950. (Supersedes NACA RM's E7B11e and E7G30.)
15. Brown, W. Byron, and Donoughe, Patrick L.: Extension of Boundary-Layer Heat-Transfer Theory to Cooled Turbine Blades. NACA RM E50F02, 1950.
16. Hubbartt, James E., and Schum, Eugene F.: Average Outside-Surface Heat-Transfer Coefficients and Velocity Distributions for Heated and Cooled Impulse Turbine Blades in Static Cascades. NACA RM E50L20, 1951.
17. Slone, Henry O., Hubbartt, James E., and Arne, Vernon L.: Method of Designing Corrugated Surfaces Having Maximum Cooling Effectiveness Within Pressure-Drop Limitations for Application to Cooled Turbine Blades. NACA RM E54H20, 1954.
18. Slone, Henry O., and Hubbartt, James E.: Analysis of Factors Affecting Selection and Design of Air-Cooled Single-Stage Turbines for Turbojet Engines. IV - Coolant-Flow Requirements and Performance of Engines Using Air-Cooled Corrugated-Insert Blades. NACA RM E55C09, 1955.
19. Slone, Henry O., and Esgar, Jack B.: Gas-to-Blade Heat-Transfer Coefficients and Turbine Heat-Rejection Rates for a Range of One-Spool Cooled-Turbine Engine Designs. NACA RM E56A31, 1956.
20. Eckert, E. R. G.: Introduction to the Transfer of Heat and Mass. First ed., McGraw-Hill Book Co., Inc., 1950.

4284

CU-3 back

TABLE I. - TABULATION OF HEAT-TRANSFER DATA

Engine speed, rpm	Effective gas temperature, °F	Blade temperatures, °F						Engine mass flow, lb/sec	Coolant-flow ratio	Blade cooling-air inlet temperature, °F
		1/3-Span				Root				
		Leading edge	Trailing edge	Midchord suction surface	Midchord pressure surface	Trailing edge	Midchord suction surface			
10,000	1131	825	880	800	812	760	642	61.96	0.0166	152
	1132	848	909	835	860	760	644	62.20	.0113	155
	1130	910	980	948	960	800	746	62.28	.0073	175
	1133	915	986	960	982	818	752	63.36	.0076	167
	1129	980	1046	1039	1060	860	842	63.26	.0066	196
	1125	1009	1072	1062	1089	882	878	63.34	.0041	215
	1130	1066	1095	1098	1028	922	930	63.14	.0032	302
11,500 (rated)	1462	----	1235	1180	1210	1025	960	73.58	0.0135	249
	1450	----	1250	1226	1250	1035	1000	73.80	.0093	258
	1459	----	1320	1309	1330	1085	1070	73.16	.0082	298
	1460	----	1370	1380	1410	1138	1185	71.94	.0063	346
	1458	----	1400	1400	1445	1200	1258	73.16	.0023	440

TABLE II. - SUMMARY OF STRUCTURAL-RELIABILITY RESULTS

[Engine speed, 11,500 rpm (rated); corrugations of A-286; 1/3-span temp., 1375° F.]

Blade material	Stress, psi		Blade	Average turbine-inlet temperature, °F	Coolant-flow ratio	Running time, hr:min		Ratio of allowable to centrifugal stress at 1/3 span	Remarks
	Base	1/3-span				Total	At test condition		
HS-31 (X-40)	33,100	28,700	2	1670	0.0064	26:16	15:52	1.40	Total running time includes approximately 10 hr at lower speeds for heat-transfer tests. No failure.
			3	1670	0.0064	35:50	30:50	1.36	No failure.
			4	1600	0	37:48	35:58	1.35	No failure.

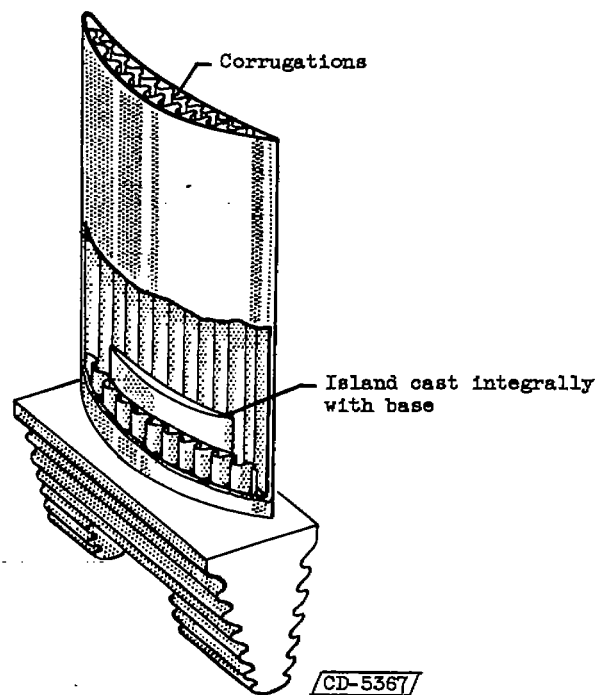
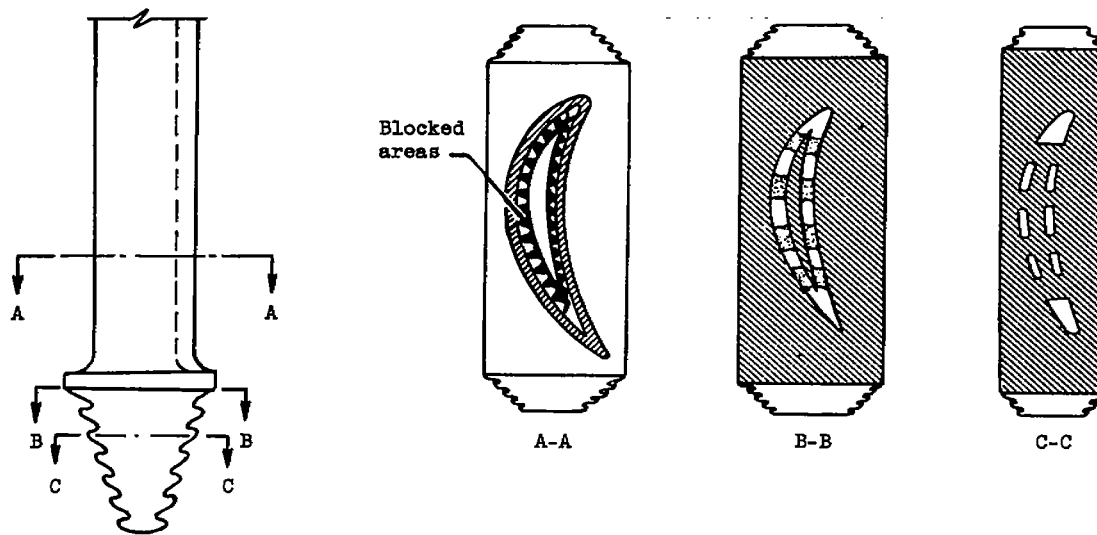


Figure 1. - Construction details of test blade with integrally cast shell and base.  
Corrugations brazed in place to augment heat-transfer surface.

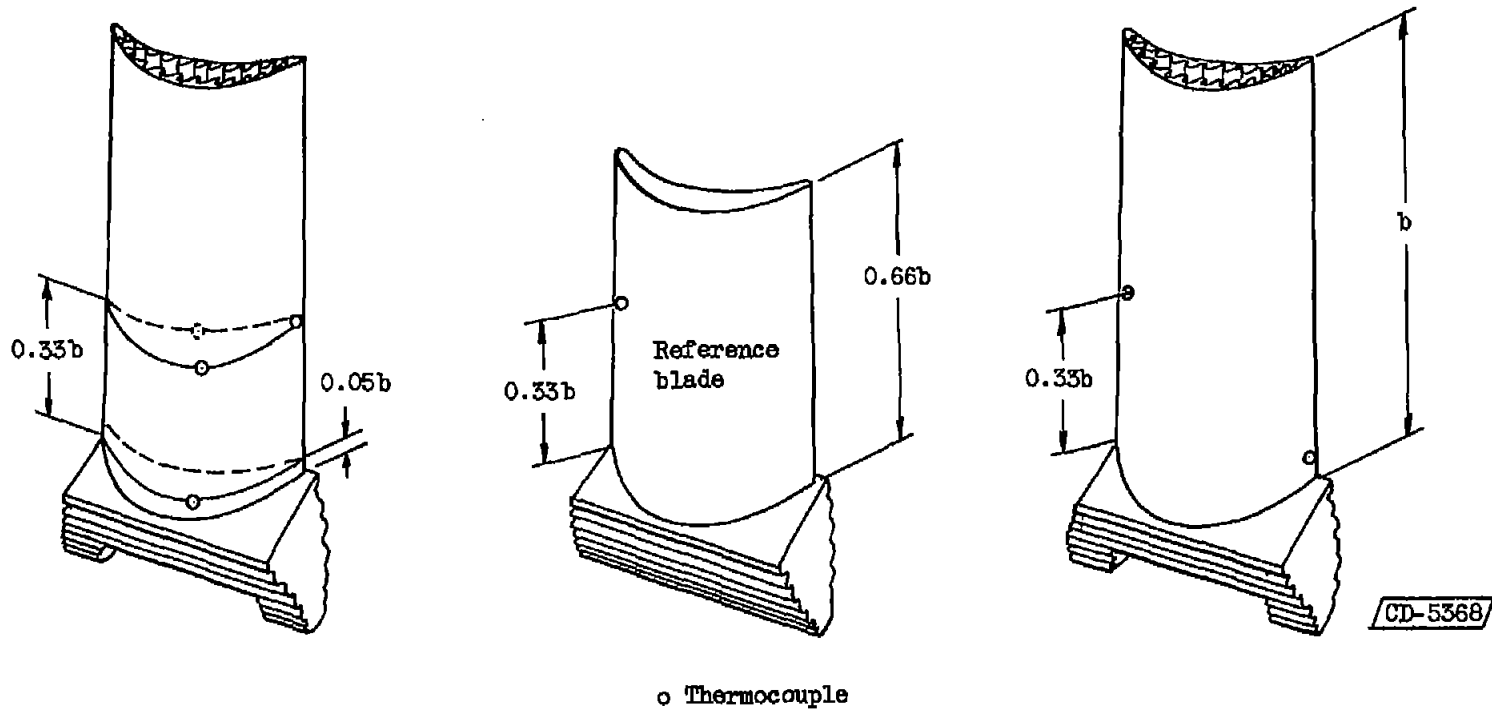
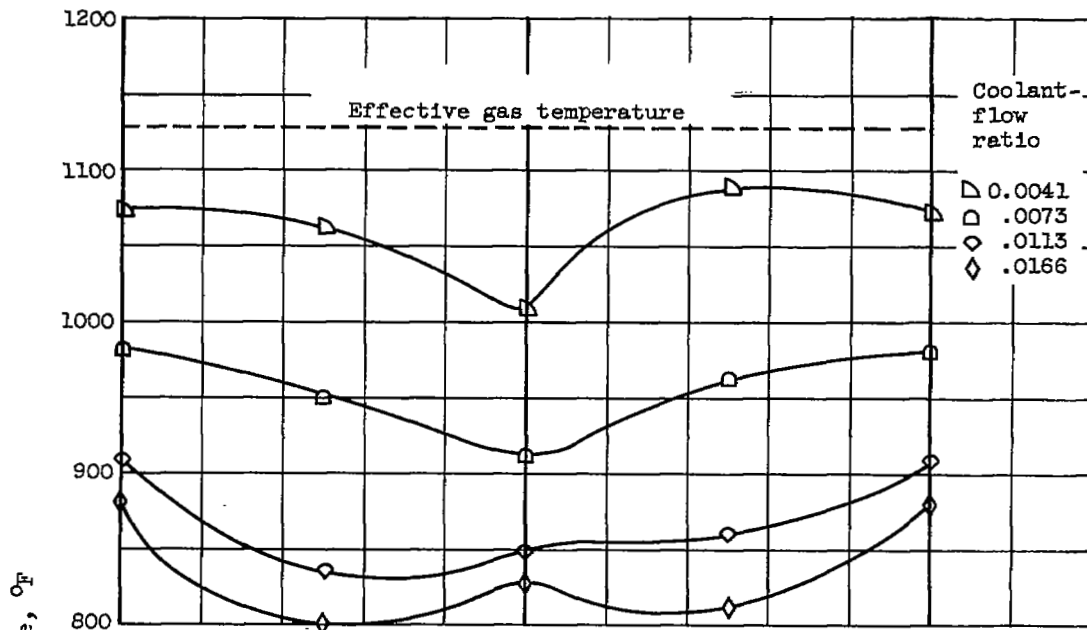
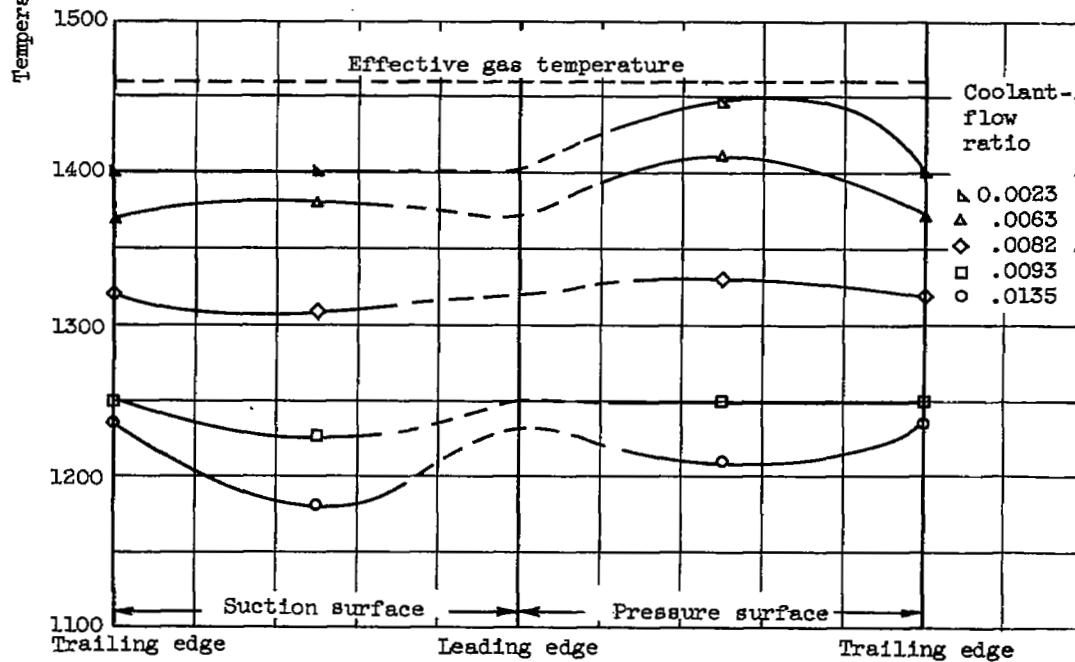


Figure 2. - Thermocouple installation on cooled and uncooled blades.



(a) Engine speed, 10,000 rpm.



(b) Engine speed, 11,500 rpm (rated).

Figure 3. - Chordwise temperature distributions for modified corrugated-insert blade at 1/3-span position. (Cooling-air inlet temperatures given in table I.)

4284

CJ-4

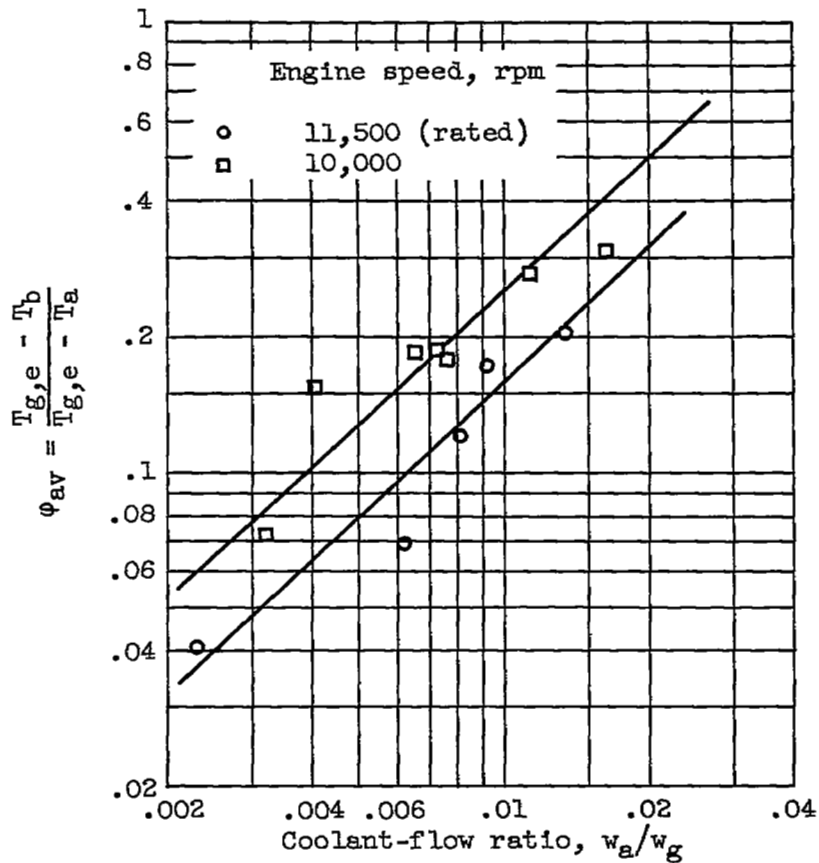


Figure 4. - Nondimensional cooling effectiveness parameter (based on av. 1/3-span blade temperature) as function of coolant-flow ratio at two engine speeds for modified corrugated-insert blade.

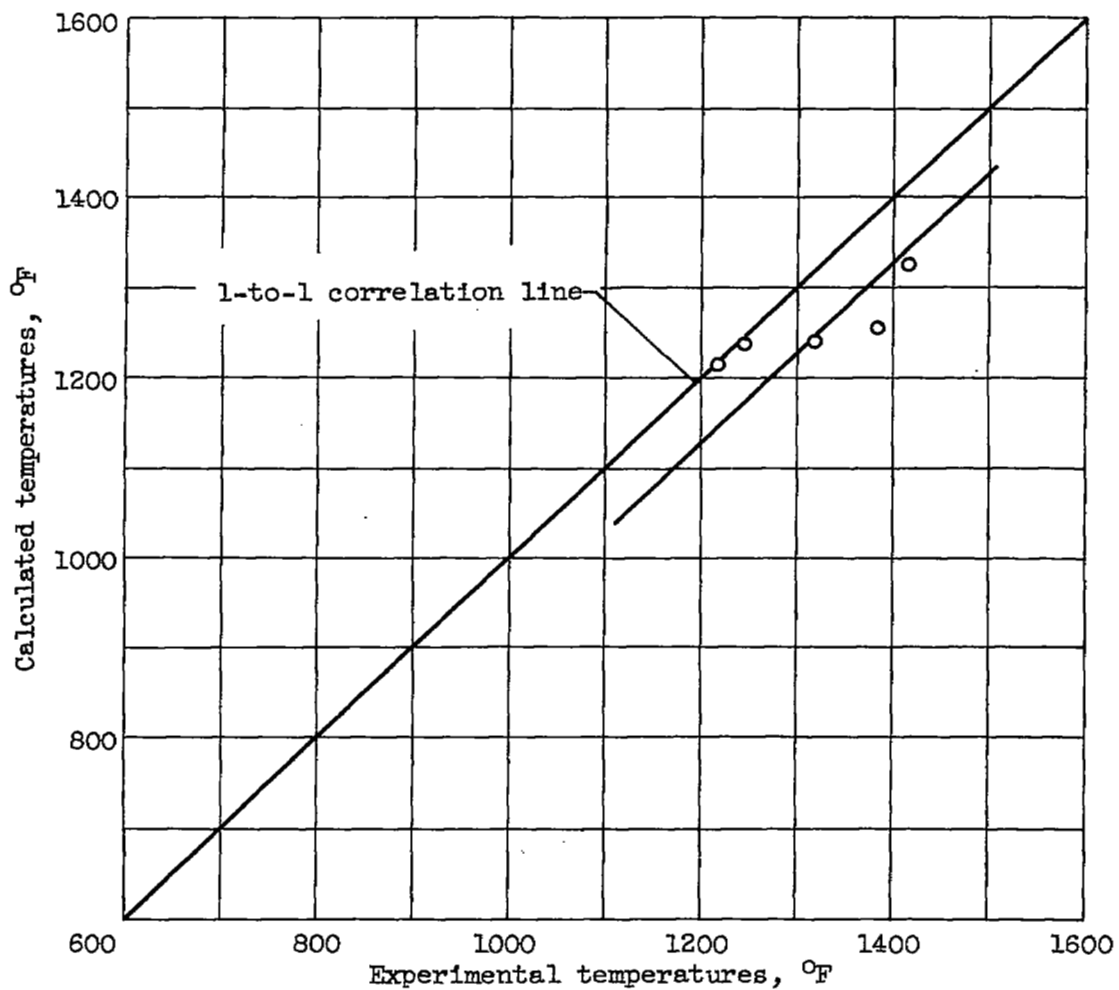
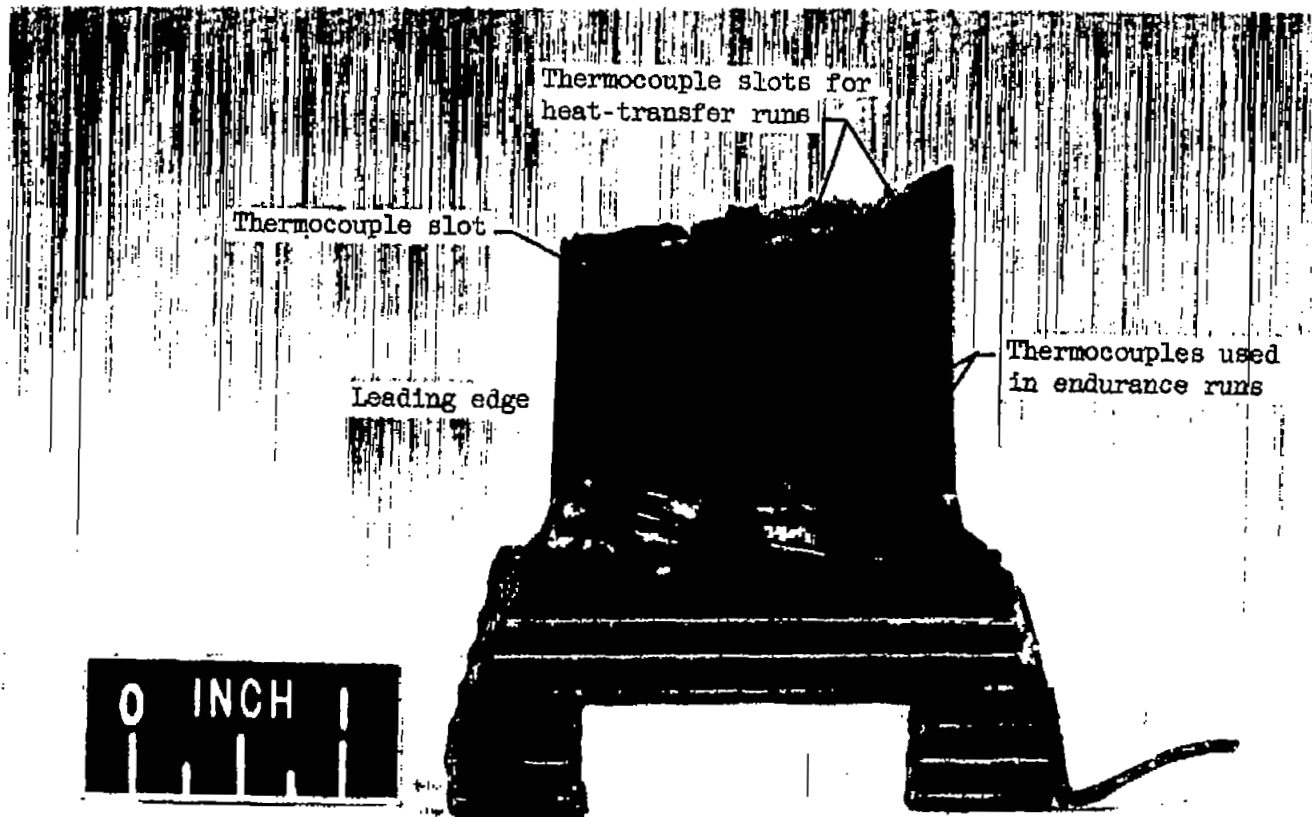


Figure 5. - Comparison of calculated and experimental 1/3-span average blade temperatures for modified corrugated-insert blade. Coolant-flow-ratio range, 0.0023 to 0.0135; inlet gas temperature, 1670° F; engine speed, 11,500 rpm.



C-41663

Figure 6. - Failed HS-21 blade.

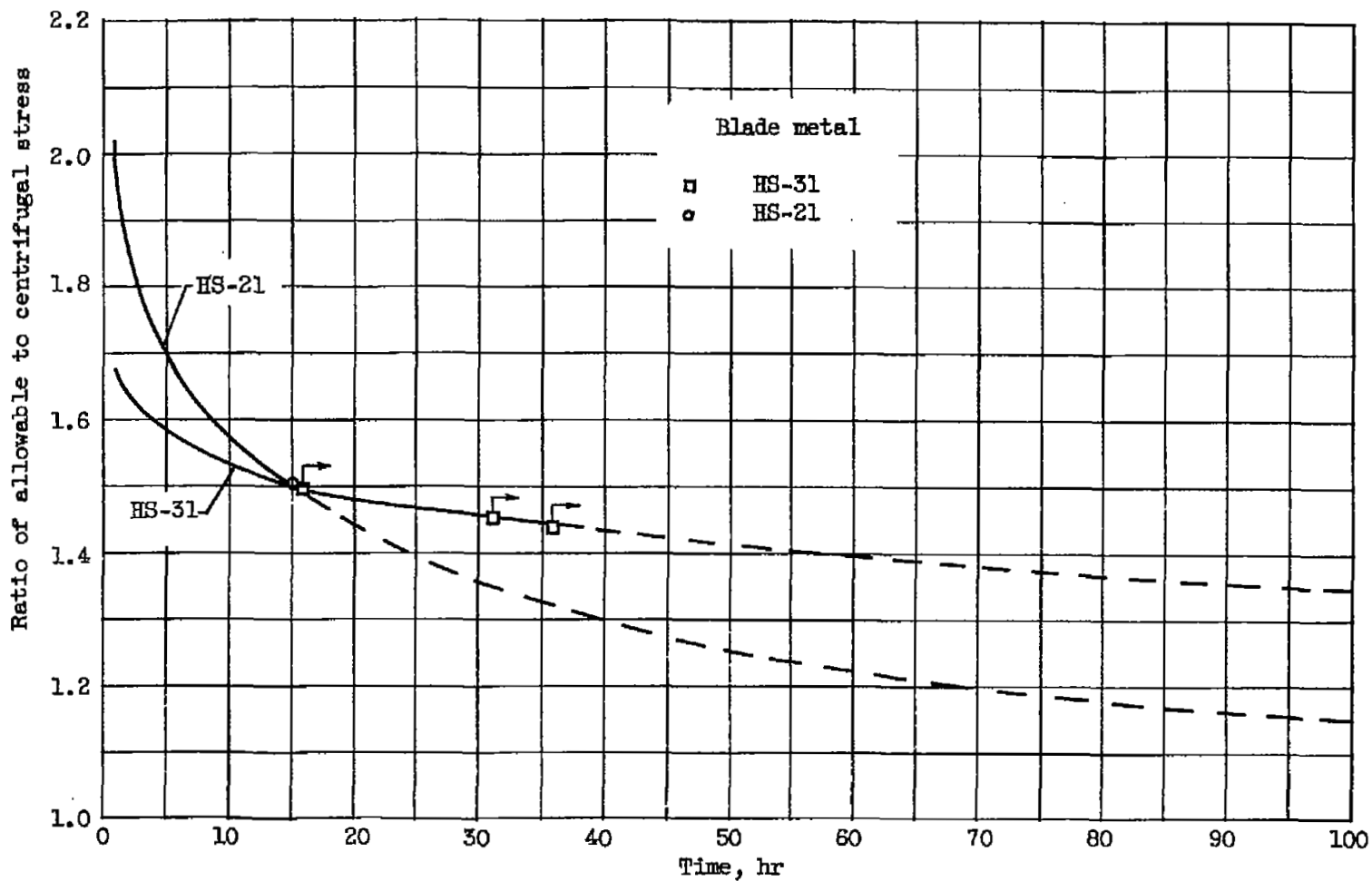


Figure 7. - Ratio of allowable to centrifugal stress at 1/3-span as function of time for blades investigated at an average 1/3-span blade temperature of 1375° F.

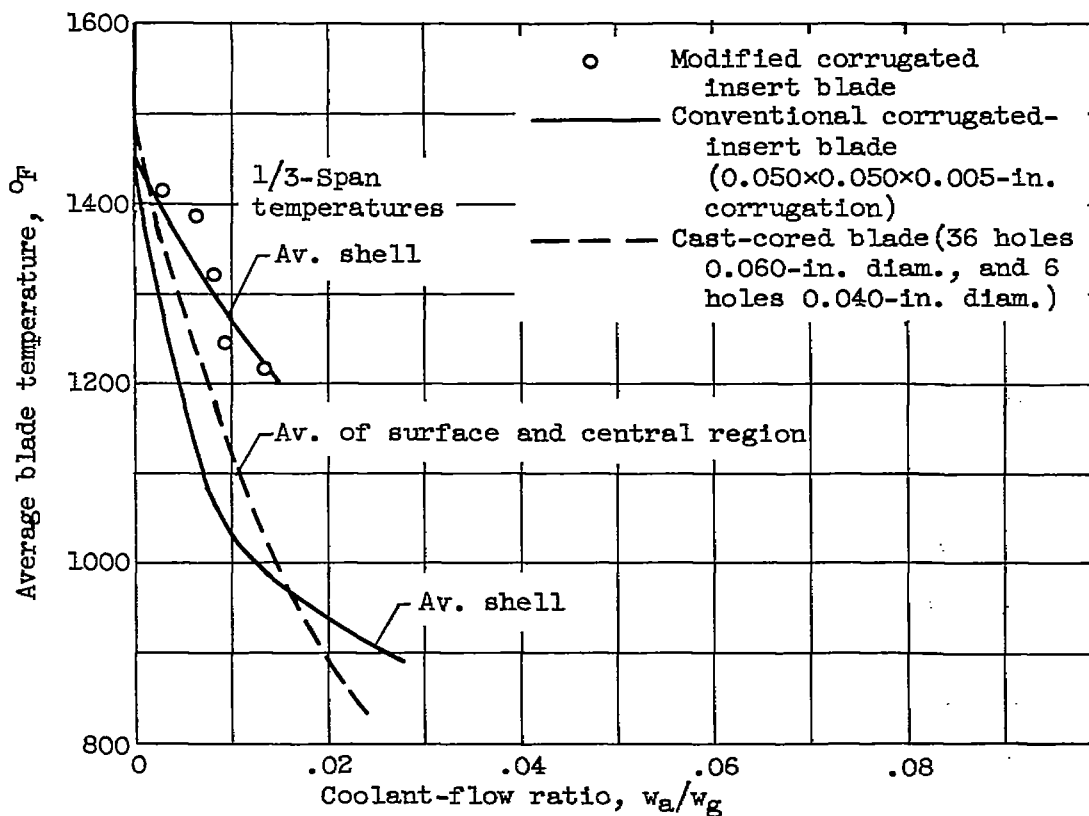


Figure 8. - Change in average blade temperatures with coolant-flow ratio at 1/3-span position at rated engine conditions (1670° F turbine-inlet temp., 11,500 rpm) for several air-cooled blade configurations.

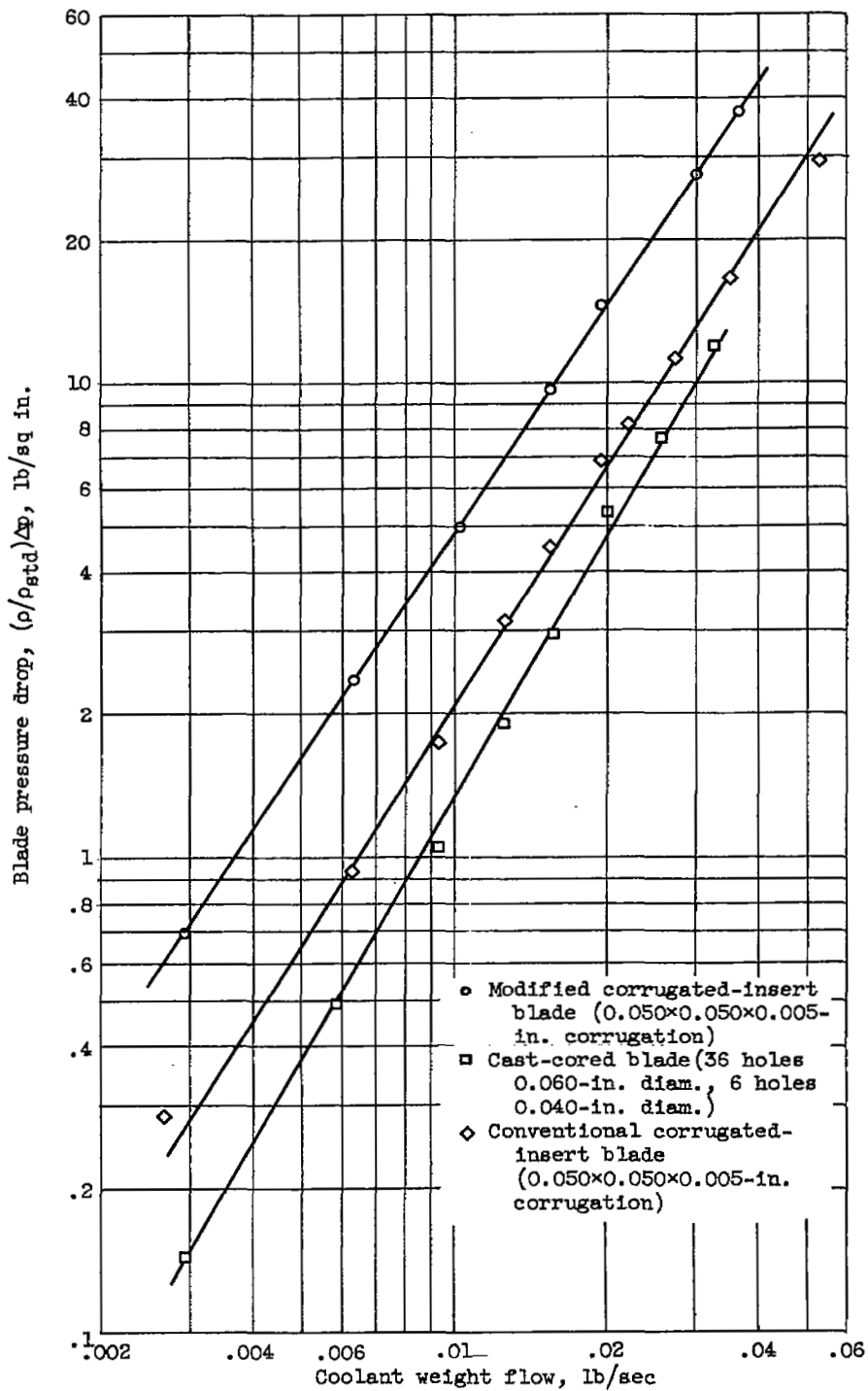


Figure 9. - Change in blade pressure drop with coolant weight flow for several air-cooled blade configurations.

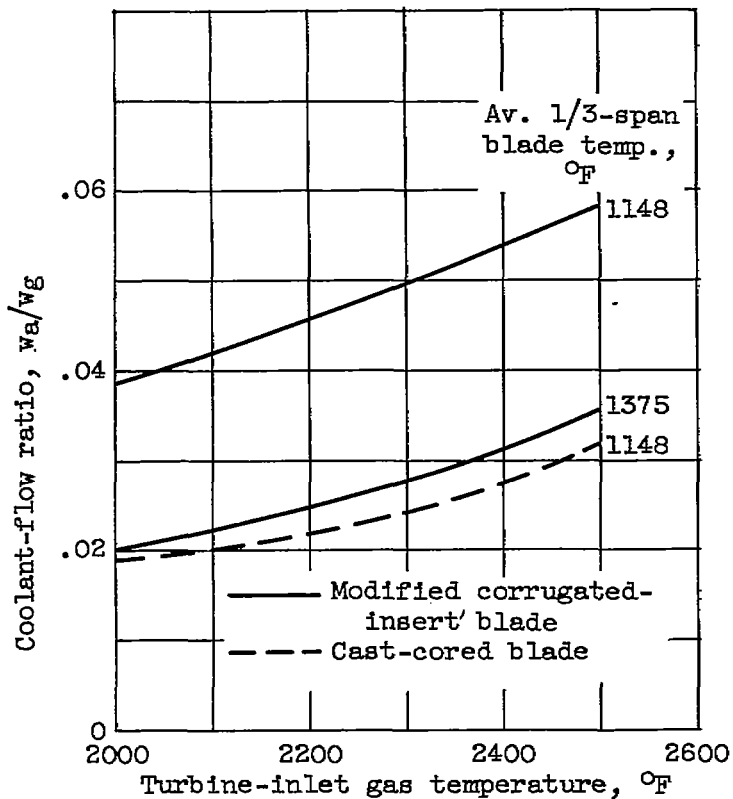
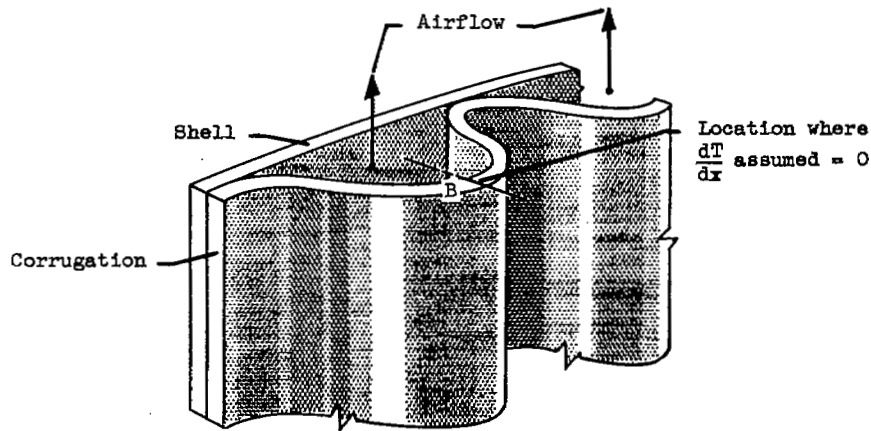
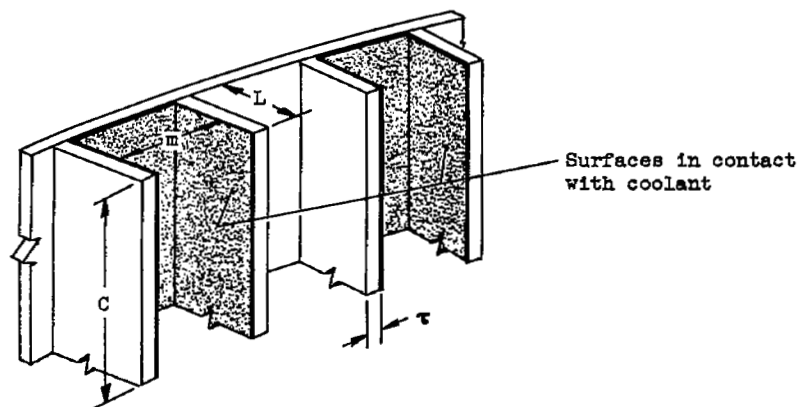


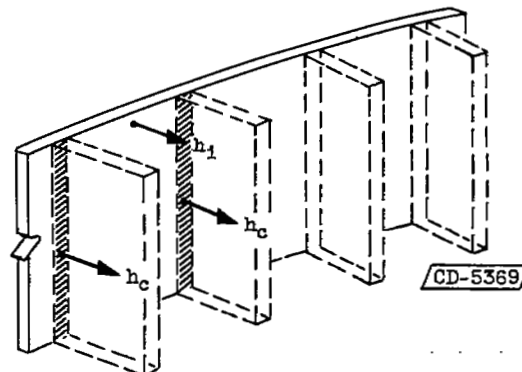
Figure 10. - Calculated variation of coolant-flow ratio with inlet gas temperature for modified corrugated-insert and cast-cored blades. Altitude, 50,000 feet; flight Mach number, 2.



(a) Portion of shell with attached corrugations.



(b) Equivalent configuration.



(c) Substitution of heat-transfer coefficients for cooling action of equivalent fins.

Figure 11. - Sketch showing simplified configuration equivalent to corrugation used in this analysis.

NASA Technical Library



3 1176 01436 0862

